Radio Science, Volume 33, Number 3, Pages 707–717, May–June 1998

Ground-based microwave radiometry and long-term observations of atmospheric water vapor

Gunnar Elgered and Per O. J. Jarlemark[1]

Onsala Space Observatory, Chalmers University of Technology, Onsala, Sweden

Abstract. Microwave radiometer data and radiosonde data from the time period 1981–1995 have been used to study long-term trends in the integrated precipitable water vapor (IPWV). The two instruments have operated 37 km apart on the Swedish west coast. Model parameters are estimated for the entire data sets as well as for subsets of the data. The IPWV model parameters are a mean value, a linear drift with time, and the amplitude and phase of an annual component. The radiosonde data, which are uniformly sampled in time, show an increase in the IPWV of 0.03 mm/yr with a statistical standard deviation of 0.01 mm. The microwave radiometer data, which are not at all uniformly sampled in time, show -0.02±0.01 mm/yr. We show that the disagreement is caused by the different sampling of the data for the two instruments. When the two data sets are reduced to include only data that are sampled simultaneously, we find an agreement between all estimated model parameters, given their statistical uncertainties. This suggests that if the microwave radiometer had also been operating continuously over the 15-year period, its data would have implied a linear trend similar to the result obtained from the radiosonde data. The general quality of the data, in terms of the short time scatter, has been improved over the time period. The root mean square (RMS) difference between the IPWV measured by the radiometer and by the radiosondes was 2.1 mm during the first 5 years and was reduced to 1.6 mm during the last 4 years. These values include the real difference in the IPWV between the two sites. The bias, radiometer-radiosonde, was 0.1 mm for the whole data set and varied between -0.2 and 0.9 mm for smaller data sets of a few years.

1. Introduction

Atmospheric water vapor plays an important role in the energy balance of the Earth [*Rasool and De Bergh*, 1970]. The "greenhouse" effect has been quantitatively estimated using satellite-borne instruments operating in both the microwave and the infrared parts of the electromagnetic spectrum [*Raval and Ramanathan*, 1989; *Rind et al.*, 1991].

The integrated precipitable water vapor (IPWV) is a useful probe when searching for possible trends in the Earth's climate. Furthermore, a major difficulty in climate modeling is the treatment of clouds [*Cess et al.*, 1990; *Chen and Roeckner*, 1996], an effect closely related to variations in the IPWV. Radiosonde data covering time periods of 10 years or more have been used to estimate trends in the IPWV of the atmosphere [*Gaffen et al.*, 1992]. An accurate documentation of the calibration history of the humidity and temperature sensors is necessary in order to draw any conclusions from these apparent trends, since the estimated trends are relatively small; over a decade it is typically less than the reproducibility of the humidity sensor as specified by the manufacturer. (See, for example, *England et al.* [1993] and *Wade* [1994] for a discussion on errors of different types of radiosondes.) The situation can be improved if an independent technique is used to measure the IPWV accurately and thereby validate the radiosonde data.

[1]Now at Harvard-Smithsonian Center for Astrophysics, Cambridge, Massachusetts.

Paper number 98RS00488.
0048-6604/98/98RS-00488$11.00

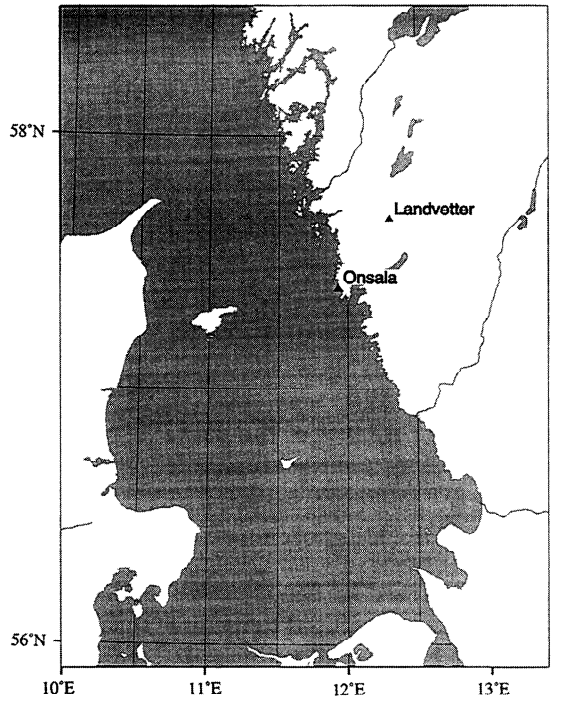

Figure 1. A part of the Swedish west coast showing the water vapor radiometer (WVR) site, Onsala, and the radiosonde launching site, Landvetter. The distance between the sites is 37 km.

During the last few years, continuously operating, ground-based Global Positioning System (GPS) receivers have been put into operation. Global as well as regional networks with the possibility of producing continuous time series of the IPWV exist today [*Beutler et al.*, 1996; *Tsuji et al.*, 1995; *Dragert and Hyndman*, 1995; *BIFROST Project*, 1996]. These networks of GPS receivers will provide a better spatial and temporal resolution compared with the existing network of radiosonde stations [*Businger et al.*, 1996] and have the potential to become an important tool for climate studies. The GPS technique suffers, of course, from deficiencies in models used in the geodetic data analysis. Therefore it is of fundamental importance to have different methods to investigate the quality of the results. One instrument capable of producing IPWV estimates is a ground-based microwave radiometer, hereinafter referred to as a water vapor radiometer (WVR) [see, e.g., *Hogg et al.*, 1983, *Elgered*, 1993, and references therein].

With this application in mind, but also the possibility of using the WVR as a stand-alone instrument, this study assesses the long-term accuracy of the IPWV estimated from the WVR data. We start with an archived data set of the estimated radio wave propagation delay caused by the atmospheric water vapor, simply called the wet delay. In the following we will always use the equivalent zenith value for this quantity. In our data set, including observations at elevation angles above 18°, a simple cosecant law can be used to "map" observations to the zenith. If observations are made at elevation angles at say 15° or lower more sophisticated "mapping functions" must be used [see *Niell* 1996 and references therein].

In section 2 we review the relationship between the wet delay and the IPWV. We compare the WVR data acquired at the Onsala Space Observatory on the Swedish west coast with data from radiosondes, launched at Landvetter Airport, 37 km away, for the time period 1981–1995. The instruments, the data set, and the data analysis are described in section 3. The results are found in section 4, where we compare the estimated trends in the IPWV for the two methods at the two sites. We also present the RMS differences between the two time series of simultaneously sampled data. The conclusions appear in section 5.

2. Background Theory

Our 15 year-long WVR data set consists of archived time series of the wet delay. We will briefly summarize here the relation between this quantity and the atmospheric water vapor content. The wet delay in the zenith direction is presented here in units of length as an apparent excess propagation path (compared with the case of propagation in vacuum) [*Elgered*, 1993]:

$$\ell_w = (0.382 \pm 0.004) \int_0^\infty \frac{e}{T^2} Z_w^{-1} \, dh \qquad (1)$$

where e is the partial pressure of water vapor in millibars; T is the temperature in kelvins; and Z_w is a correction factor (close to unity) for departures from the ideal gas law. The uncertainty of ± 0.004 takes into account the experimental uncertainties in physical constants and an uncertainty of 20 K in the effective atmospheric temperature T_m. The atmospheric water vapor content is a related quantity since it is the integral of the water vapor density profile in the atmosphere. It is common to use the IPWV as a measure of the atmospheric water vapor content:

Table 1. Original Technical Specifications of the Water Vapor Radiometer

Parameter	Value
Frequencies	21.0 and 31.4 GHz
Antenna (one for each frequency)	dielectrically loaded horn
Antenna beam widths	6° (both channels)
Mount	azimuth (AZ) / elevation (EL)
Positioner	step motors, 0.025°/step after gearbox
Slew rate (both AZ and EL)	1.8°/s
Pointing resolution	0.1° (both AZ and EL)
Reference load temperatures, cold mode	77 and 313 K
Reference load temperatures, hot mode	313 and 360 K
System noise temperature 21.0 GHz	~450 K
System noise temperature 31.4 GHz	~550 K
RF bandwidth (both channels)	~1 GHz
Accuracy (both channels)	~1 K

$$\mathrm{IPWV} = \frac{1}{a_w} \int_0^\infty a_v(h)\, dh \tag{2}$$

where a_v is the density of water vapor in g/m^3 as a function of the height h in meters and a_w is the density of water (1.0×10^3 kg/m^3). These units yield IPWV in millimeters. Using the ideal gas law to combine (1) and (2), we obtain the relation

$$\frac{\ell_w}{\mathrm{IPWV}} = \frac{1763}{T_m} \tag{3}$$

where both ℓ_w and IPWV are in the same unit of length (e.g., millimeters) and where the effective mean temperature T_m in kelvins is

$$T_m = \frac{\int_0^\infty \frac{e}{T} Z_w^{-1}\, ds}{\int_0^\infty \frac{e}{T^2} Z_w^{-1}\, ds} \tag{4}$$

We note that the wet delay and the IPWV are strongly correlated, related by a factor which is proportional to an "effective mean" temperature of the atmosphere obtained by weighting the temperature with the wet refractivity ($\propto e/T^2$). For an effective mean temperature of 270 K, for example, a wet delay of 6.5 mm corresponds to an IPWV of 1 mm. For a more detailed discussion, see, for example, *Bevis et al.* [1992].

3. Instrumentation and Data Analysis

The data used were acquired from WVR measurements at the Onsala Space Observatory and radiosonde launches at the Landvetter Airport on the Swedish west coast. The locations of these sites are shown in Figure 1.

The WVR was primarily designed and built to support space geodetic measurements using very-long-baseline interferometry (VLBI) [*Elgered et al.*, 1991]. It has also been used to support high precision geodetic surveying using the Global Positioning System (GPS) [*Johansson*, 1992, *Dodson et al.*, 1996]. Since the summer of 1993 the instrument has been operating in a continuous "sky-mapping" mode, logging some 5000 data points per day. The original spec-

Table 2. Important Events Within the Time Period of the Data Set

Date	Event
Dec. 20, 1985	first RS80 radiosonde launched at Landvetter
March 17, 1986	last RS18 radiosonde launched at Landvetter
May 31, 1988	WVR elevation controlled by a mirror
Feb. 10, 1992	major WVR upgrade (elevation range increased to 0°–180°; slewing speed increased to 8°/s; cold load removed; hot load temperature increased to ~375 K; hot load improved stability <0.01 K/h; resolution of the A/D converter improved ~0.02 K)

WVR, water vapor radiometer.

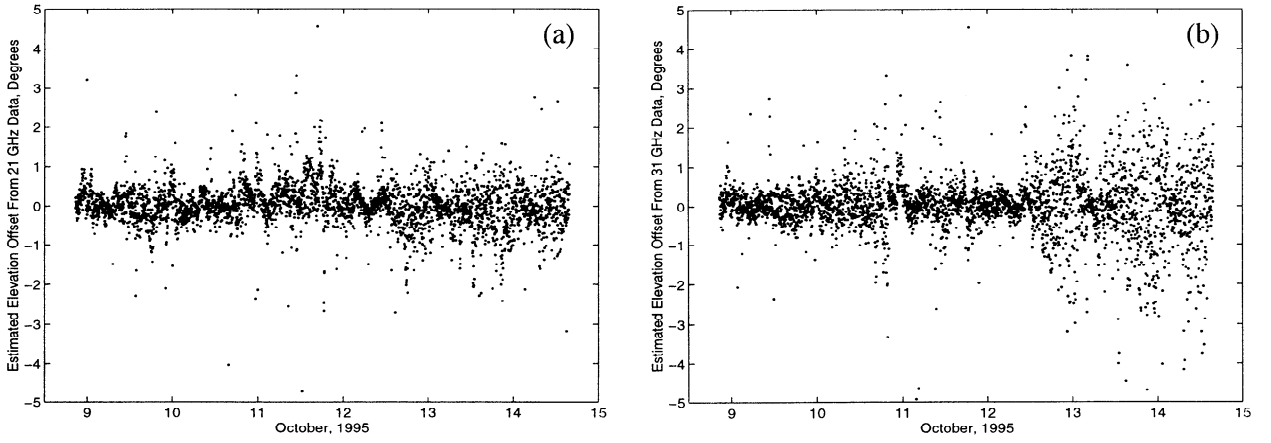

Figure 2. An example of estimated elevation offset using tip curve data at (a) 21.0 GHz and (b) 31.4 GHz. The observed scatter is caused by atmospheric inhomogeneities. The increased scatter observed during the final 2–3 days is most likely caused by the presence of liquid water, since the scatter is largest at the 31.4 GHz channel. For this data set an average of the estimated offsets is 0°, and hence no elevation angle correction is applied in the analysis.

ifications of the instrument are shown in Table 1. Several upgrades of the instrument have been carried out. The software used is quite different today compared with the original version of 1980. These upgrades have enabled a higher flexibility in the data acquisition as well as in the pointing of the radiometer. The accuracy has been improved, and the slewing speed has been increased. The WVR improvements and the corresponding dates are listed in Table 2. These dates are later used to divide the data into smaller data sets. The WVR has no independent readout of the pointing, which is only monitored by counting the pulses sent to the step motors. The mirror for elevation control was introduced to increase

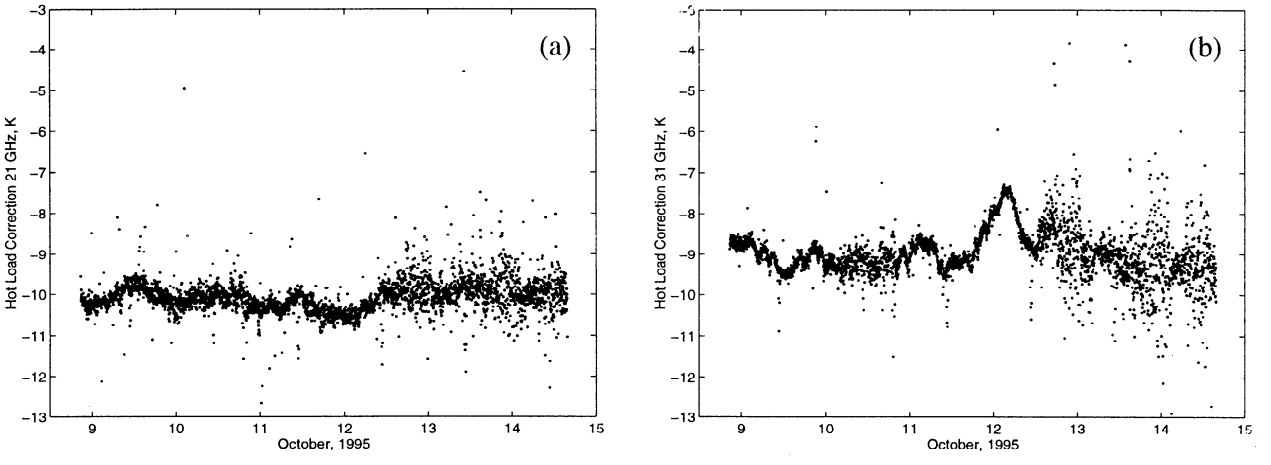

Figure 3. Estimated corrections to the hot reference loads in (a) the 21.0-GHz channel and (b) the 31.4-GHz channel. These estimates are more uncertain when liquid water is present in the atmosphere (compare with Figure 2). The statistical standard deviation (not shown) of a single data point is typically between 0.1 and 0.5 K during the periods with low scatter when 10–20 observations are included in the tip curve analysis but can increase to many kelvins depending on the inhomogenity of the sky emission.

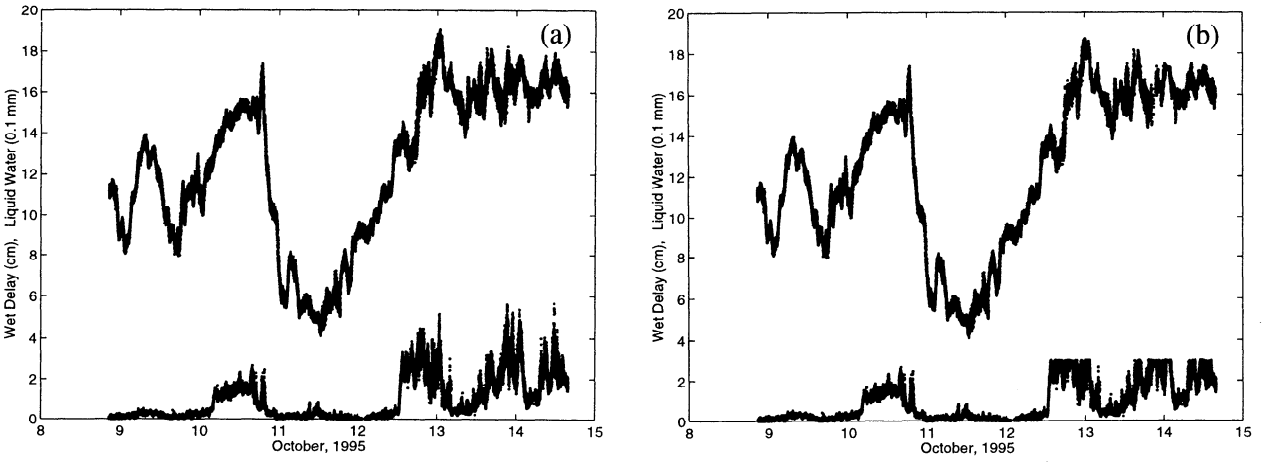

Figure 4. The wet delay and the liquid water content inferred from measurements with the WVR at the Onsala Space Observatory. Figure 4a shows the wet delay time series (upper curve) using the standard 0.7-mm cutoff for the acceptable amount of liquid water (lower curve), and Figure 4b shows the wet delay (upper curve) when this cutoff in the liquid water (lower curve) is reduced to 0.3 mm. The number of data in this case are reduced from 41,499 to 38,866.

the mechanical stability of the pointing, compared with the previous mount of the whole microwave unit in a fork, which was affected by strong winds.

The WVR data analysis can be described as a continuous "tip curve" analysis, where every data point and its corresponding elevation angle are used to solve for instrumental corrections. These data can be used to estimate a possible pointing offset for the elevation coordinate as well as corrections to the temperature of the reference loads in the radiometer.

The estimates of a pointing offset could only be accomplished with a reasonable accuracy after 1992 when the WVR could make observations from horizon to horizon. However, in practice, an elevation limit of approximately 20° is used to avoid ground noise pick-up by the sidelobes of the antenna beams. An example of estimated pointing offsets for the two channels is shown in Figure 2. For this data set a

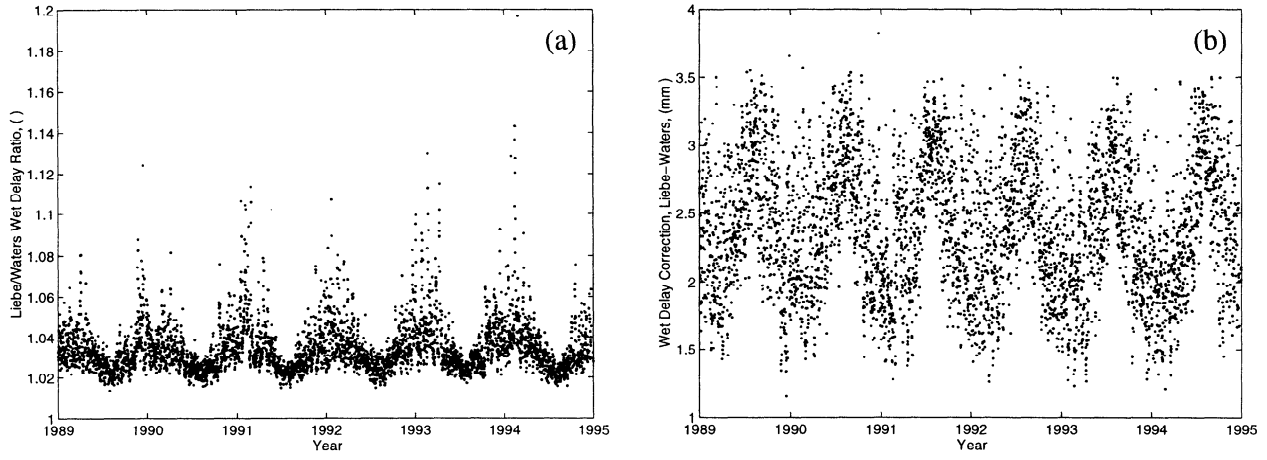

Figure 5. A comparison of wet delay calculated using two different retrieval algorithms from a set of simulated antenna temperatures (see text): (a) the ratio between wet delays based on *Liebe's* [1992] and *Waters'* [1976] attenuation coefficients and (b) the absolute value of the difference.

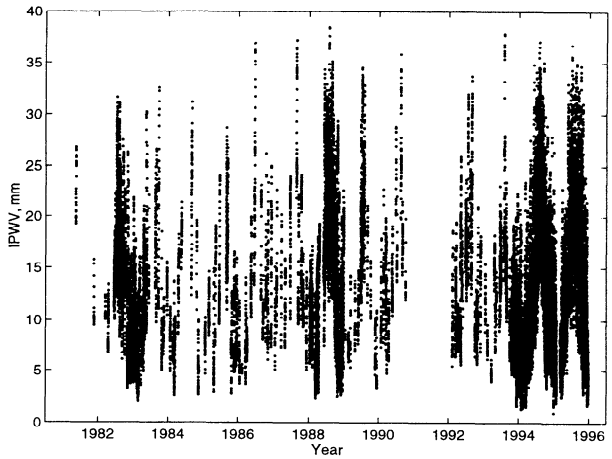

Figure 6. The integrated precipitable water vapor (IPWV) inferred from WVR observations at the Onsala site. In total, there are 30,967 data points. Each one is an averaged value using a Gaussian window with a full width half maximum of 1 hour.

mean value is used. When occasional failures in the pointing occur, most often because of missed steps of the motors, as is evidenced from the estimated offsets, the data set is divided into subsets using different pointing offsets. Pointing offsets can also be introduced when the positioner is calibrated by activating limit switches at the end points of the elevation interval if these are suffering from mechanical instabilities. Because these problems the WVR positioner was frequently calibrated during the first 10 years (at least monthly in connection with VLBI experiments) when it was not possible to obtain accurate estimates of the elevation offset. Therefore systematic effects due to pointing errors are likely to vary with a timescale of a month or less during this period.

Empirical corrections to the hot reference load in each channel are estimated from the tip curves when the elevation offset has been determined. An example of such corrections is shown in Figure 3. Using this method, the WVR obtains its absolute calibration of the measured sky emission [*Elgered*, 1993]. These corrections are believed to track temperature variations within the WVR but the results from a specific tip curve are, of course, affected by possible atmospheric inhomogeneities. Therefore a final time series of corrections is obtained by smoothing these data using a Gaussian window with a full width half maximum (FWHM) of typically 2–4 hours. The one-sigma uncertainties of the tip-curve corrections are not shown in Figure 3. They are obtained by requiring that the χ^2 per degree of freedom in each tip curve be equal to unity. After smoothing the data in Figure 3 the resulting hot load correction has a statistical uncertainty between 0.01 and 0.1 K, depending on the scatter. Thereafter the observed sky brightness temperatures are calculated and used in a retrieval algorithm for calculating the wet delay [*Elgered*, 1993]. The wet delay time series for our example data set is shown in Figure 4.

The retrieval algorithm for WVR data acquired during rain has poor accuracy. Therefore, when the WVR observations imply a liquid water content larger than 0.3 mm, the data are discarded. When comparing Figures 4a and 4b, it is seen that for this data set this upper limit of 0.3 mm could have been increased without affecting the wet delay time series dramatically. We are here, however, concerned with trends in the wet delay (and in the IPWV). It is likely that relatively more observations are carried out under high liquid water conditions during the last 3 years, when the WVR was running continuously, compared with the earlier data sets, which were often obtained during more favorable conditions. Therefore we chose this low limit of 0.3 mm of liquid water in order to reduce possible systematic effects in the data set.

The retrieval algorithm used for the data before 1992 was based on models for the attenuation coefficient of water vapor described by *Waters* [1976].

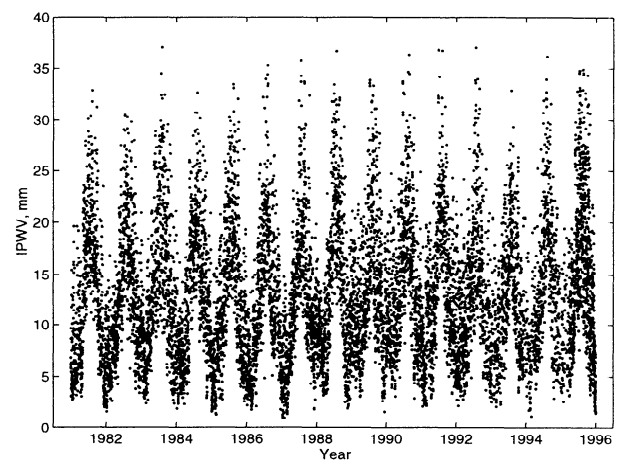

Figure 7. The integrated precipitable water vapor (IPWV) derived from the radiosonde data. In total there are 10,507 launches from this time period included in the analysis.

Table 3. Estimated Parameters for Modeling Long-Term Variations in the Integrated Precipitable Water Vapor Using the Entire WVR and Radiosonde Data Sets

Data Set	Number of Data	a_1, mm	a_2, mm/yr	a_3, mm	a_4, mm
All RS (1981–1995)	10,507	12.75±0.09	0.03±0.01	-3.06±0.07	-5.46±0.07
All WVR (1981–1995)	30,967	13.34±0.07	-0.02±0.01	-3.13±0.04	-5.58±0.04
RS, Jan. 1981 to Dec. 1985	3,490	12.81±0.15	-0.01±0.05	-3.10±0.11	-5.92±0.11
WVR, Jan. 1981 to Dec. 1985	6,089	13.31±0.14	-0.23±0.05	-2.52±0.08	-5.19±0.08
RS, March 1986 to April 1988	1,541	10.77±1.16	0.28±0.18	-3.18±0.16	-5.39±0.17
WVR, March 1986 to April 1988	2,360	13.76±1.06	0.00±0.16	-3.12±0.14	-4.16±0.18
RS, May 1988 to Oct. 1990	1,682	15.46±1.63	-0.18±0.19	-2.53±0.18	-5.07±0.18
WVR, May 1988 to Oct. 1990	5,529	18.58±1.09	-0.50±0.13	-1.17±0.14	-6.41±0.10
RS, Feb. 1992 to Dec. 1995	2,674	8.84±1.12	0.30±0.08	-3.11±0.15	-5.43±0.15
WVR, Feb. 1992 to Dec. 1995	16,917	8.17±0.60	0.34±0.04	-3.57±0.06	-5.43±0.05

RS, radiosonde.

Since the major WVR upgrade, ending in January 1992, a new retrieval algorithm has been used which is based on the millimeter wave propagation model (MPM) [*Liebe*, 1992]. The two algorithms used for the two time periods are documented by *Johansson et al.* [1993] and *Jarlemark* [1994], respectively.

Ideally, the older data set should be reprocessed using the new algorithm. Although not impossible, such a task would be relatively time consuming. Instead, we decided to develop a model and make a correction to the already archived wet delay data. We calculated the wet delay using both retrieval algorithms (hereinafter referred to as the Waters and Liebe algorithms) from simulated antenna temperatures. These temperatures were calculated from 6 years of radiosonde data from the Landvetter Airport. Figure 5 shows the result. The ratio (Liebe/Waters) of the wet delay calculated by the algorithms is presented in Figure 5a, and the difference (Liebe–Waters) is presented in Figure 5b. Owing to different line strengths and different temperature dependence for the attenuation coefficient of water vapor in the two models, the relative correction can be almost 20% during the cold part of the year when the wet delay is small. We derived the following simple model for the correction using the data in Figure 5b:

$$\Delta \ell_w = 2.40 - 0.39 \times \sin\left(2\pi \frac{t}{\tau} + 0.97\right) \qquad (5)$$

where $\Delta \ell_w$ is the correction in millimeters, t is the day of the year, and τ is the number of days in the year. The root-mean-square (RMS) scatter of the residuals of the least squares fit was 0.4 mm. This correction was then applied to the wet delays archived before 1992.

Thereafter we smoothed all the wet delay data using a Gaussian window with a FWHM of 1 hour. This resulted in 30,967 hourly averages of the wet delay. Finally, the wet delay data are used to calculate the IPWV according to *Emardson et al.* [1998] using the latitude of 57.5°N

$$\frac{\ell_w}{\mathrm{IPWV}} = 6.50 + 0.15 \times \sin\left(\frac{2\pi\, t}{\tau} + 1.20\right) \qquad (6)$$

This relation has been derived using 5 years of the radiosonde data from Scandinavia to calculate both the wet delay and the IPWV for each profile. A least square analysis is thereafter used to derive the constants in the above equation as a model of T_m

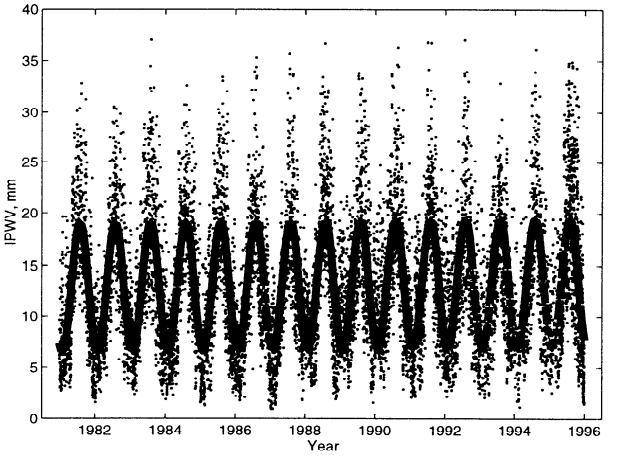

Figure 8. The radiosonde data from Figure 6 are shown together with the estimated model for the integrated precipitable water vapor (IPWV) according to equation (7) when all data are used (first entry in Table 3).

Table 4. Estimated Parameters for Modeling Long-Term Variations in the Integrated Precipitable Water Vapor Using Only Simultaneously Sampled WVR and Radiosonde Data

Data set	Number of Data	a_1, mm	a_2, mm/yr	a_3, mm	a_4, mm
All RS (1981–1995)	2141	13.08±0.25	-0.01±0.02	-3.12±0.16	-5.88±0.15
All WVR (1981–1995)	2141	13.13±0.25	0.01±0.02	-3.09±0.16	-5.58±0.15
RS, Jan. 1981 to Dec. 1985	461	13.52±0.50	-0.29±0.19	-2.82±0.29	-5.60±0.29
WVR, Jan. 1981 to Dec. 1985	461	12.71±0.48	-0.03±0.18	-2.60±0.27	-5.20±0.27
RS, March 1986 to April 1988	173	9.35±3.69	0.53±0.56	-3.22±0.50	-4.43±0.60
WVR, March 1986 to April 1988	173	13.42±3.83	0.06±0.58	-3.34±0.52	-4.19±0.63
RS, May 1988 to Oct. 1990	424	21.14±4.00	-0.85±0.49	-0.58±0.51	-6.13±0.37
WVR, May 1988 to Oct. 1990	424	18.72±3.99	-0.51±0.49	-1.00±0.51	-6.65±0.37
RS, Feb. 1992 to Dec. 1995	1078	8.63±2.42	0.31±0.18	-3.63±0.24	-5.71±0.23
WVR, Feb. 1992 to Dec. 1995	1078	8.65±2.37	0.30±0.17	-3.62±0.24	-5.59±0.23

(see equations (3) and (4)). The residuals of the fit have an RMS value of 1%. The entire IPWV data set obtained from the WVR is presented in Figure 6.

The radiosonde launching site at the Landvetter Airport is operated by the Swedish Meteorological and Hydrological Institute (SMHI). Ballons are typically launched twice per day at 0000 and 1200 UT, but occasional launches are also made at 0600 and 1800 UT. The type of radiosonde launched during the beginning of the studied time period (see Table 2) was the Vaisala RS18. The humidity sensor of this instrument, a hair hygrometer, has a specified RMS repeatability of ±3%. This radiosonde was gradually replaced by the RS80, which has a different type of sensor with a significantly better specification, namely, a repeatability of <2% and a reproducibility of <3% (J. Hörhammer, Vaisala Oy, personal communication, 1997).

Both types of radiosondes produced profiles of pressure, temperature, and humidity. These data were used to calculate the profile of the absolute humidity, which was integrated numerically according to (2). The time series of IPWV is shown in Figure 7.

4. Results and Discussion

We have carried out two different analyses of the WVR and radiosonde data sets. First, we use the entire data set from each instrument separately. We searched for systematic trends with time by estimating a linear drift. Owing to the sparse sampling of WVR data during long periods, it was necessary to model the seasonal variation by also estimating an annual frequency term. Using the method of least squares, we estimated the parameters a_i in the model

$$\mathrm{IPWV} = a_1 + a_2 \times t + a_3 \sin(2\pi t) + a_4 \cos(2\pi t) \quad (7)$$

where t is the time in years since January 1, 1981. The values of the estimated parameters are listed in Table 3. Each parameter is specified together with a statistical standard deviation. This was obtained by making the χ^2 per degree of freedom of the least squares fit to (7) equal to unity.

Figure 8, presenting the radiosonde data and the estimated model for the whole period, shows large deviations between the model and the data. Furthermore, we all know from everyday weather experiences that a period of a few weeks can be exceptionally warm and humid and the next few weeks can be unusually cold and dry. The differences, sometimes of many standard deviations, between the estimated

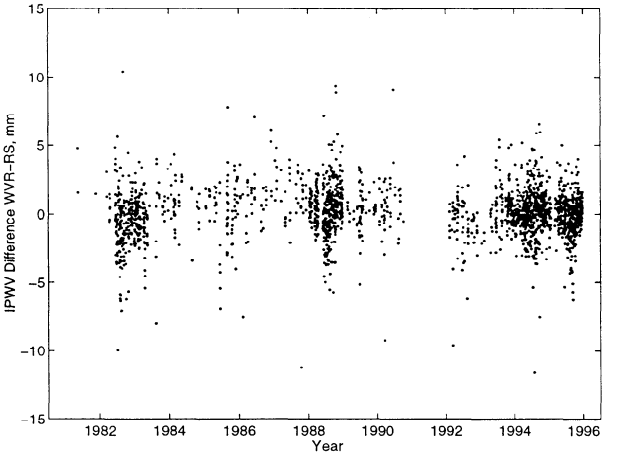

Figure 9. Differences in the IPWV measured by the WVR at the Onsala site and by radiosondes at the Landvetter Airport.

Table 5. Differences Between the Integrated Precipitable Water Vapor Measured With the WVR at the Onsala Site and With Radiosondes at the Landvetter Airport

Data set	Number of Data Pairs	Mean Difference (WVR–RS), mm	Standard Deviation mm	RMS Difference[a] mm
All (1981–1995)	2141	0.1	1.9	1.9
Jan. 1981 to Dec. 1985	461	-0.2	2.1	2.1
March 1986 to April 1988	173	0.9	1.7	1.9
May 1988 to Oct. 1990	424	0.3	2.0	2.0
Feb. 1992 to Dec. 1995	1078	0.1	1.6	1.6

[a](RMS difference)^2 = (mean difference)^2 + (standard deviation)^2

model parameters using radiosonde and WVR data in Table 3 are therefore suspected to be caused by the irregular sampling of the WVR data (compare Figures 6 and 7).

To eliminate this problem, for the instrumental comparison, a second analysis was made by identifying pairs of WVR and radiosonde estimates which were closer in time than half an hour. Table 4 summarizes the result for the whole data set, as well as for the shorter time periods as in the previous comparison in Table 3. The consistency between the model parameters using the two instruments is now acceptable for all parameters and time periods, suggesting that both instruments mainly suffer from errors which vary over short timescales. We do note, however, that the trend seen in the original radiosonde data is not detected using this smaller amount of data.

The differences observed in the IPWV between these simultaneously sampled data sets are shown in Figure 9. We calculated the mean difference, the standard deviation, and the RMS difference between the WVR and the radiosonde results (see Table 5). There is an overall improvement of the agreement with time. It is worth noting that the observed difference also includes the real spatial difference between the two sites. Assuming that the variations in the IPWV can be described as a random walk with a variance of 5×10^{-4} mm^2/s (corresponding to a variance of 2×10^{-8} m^2/s for the wet delay) which is a typical value for the Onsala site [*Jarlemark et al.*, this issue], and that the wet delay variations are caused by a "frozen flow" carried by a typical wind speed of 10 m/s, we roughly estimate the real RMS variation in IPWV between the two sites to be of the order of 1.4 mm, which agrees with the result from the analysis.

5. Conclusions

We have shown that ground-based microwave radiometers have a potential for long-term monitoring of the integrated precipitable water vapor (IPWV) and that the results for trends in the IPWV over time periods of years are consistent with those obtained from radiosonde launches if data are sampled simultaneously with the two instruments.

The entire radiosonde data set gives an increase in the IPWV of 0.03±0.01 mm/yr, where the uncertainty is the statistical standard deviation. Owing to the irregular sampling of the microwave radiometer data, especially during the first years, a similar trend cannot be seen in these data, even though the good agreement in Table 4 using the simultaneously sampled data set suggests that the trend detected with the radiosonde data could be real. If and when trends in IPWV are seen in microwave radiometer data, future work should address the possible influence of errors in the algorithm used. This algorithm is, for example, affected by variations in the temperature profile in the atmosphere, which therefore also needs to be monitored.

Over the 15-year period the quality of the WVR data as well as the radiosonde data have been improved. An RMS difference of 1.6 mm for 1078 data pairs acquired during 1992–1995 between radiosondes and the WVR, separated by 37 km, suggests that the reproducibility of each of the instruments is of the order of half a millimeter in the IPWV.

Variations in the IPWV are strongly correlated with the greenhouse effect [*Raval and Ramanathan*, 1989]. The result reported here, however, has little impact on climate modeling. For this application, better geographical coverage is needed. It would be costly to implement this by using microwave radiometry, but it could be obtained from the existing global

networks of radiosondes and/or ground-based GPS receivers. These instruments suffer, however, from other types of errors, and an important task for microwave radiometry could be to validate results from specific sites in these networks.

Acknowledgments. We are grateful for the significant improvements of the manuscript suggested by James L. Davis and Fredrick S. Solheim. Lubomir Gradinarsky analyzed the WVR data from 1993–1995. The radiosonde data have been supplied by the Swedish Meteorological and Hydrological Institute, and we especially thank Ingemar Hedenvik for information from the radiosonde archive. This work has been supported by the Swedish Natural Science Research Council and the Swedish National Space Board.

References

Beutler, G., I.I. Mueller, and R.E. Neilan, The International GPS Service for Geodynamics (IGS): The story, in *GPS Trends in Precise Terrestrial, Airborne, and Spaceborne Applications*, edited by G. Beutler et al., pp. 3–13, Springer Verlag, New York, 1996.

Bevis, M., S. Businger, T.A. Herring, C. Rocken, R.A. Anthes, and R.H. Ware, GPS meteorology: Remote sensing of atmospheric water vapor using the Global Positioning System, *J. Geophys. Res., 97*, 15,787–15,801, 1992.

BIFROST Project, GPS measurements to constrain geodynamic processes in Fennoscandia, *Eos Trans. AGU, 77*, 337–341, August 27, 1996.

Businger, S., S.R. Chiswell, M. Bevis, J. Duan, R.A. Anthes, C. Rocken, R.H. Ware, M. Exner, T. VanHove, and F.S. Solheim, The promise of GPS atmospheric monitoring, *Bull. Am. Meteorol. Soc., 77*, 5–18, 1996.

Cess, R.D., et al., Intercomparison and interpretation of climate feedback processes in 19 atmospheric general circulation models, *J. Geophys. Res., 95*, 16,601–16,615, 1990.

Chen, C.-T., and E. Roeckner, Validation of the Earth radiation budget as simulated by the Max Planck Institute for Meteorology general circulation model ECHAM4 using satellite observations of the Earth Radiation Budget Experiment, *J. Geophys. Res., 101*, 4269–4287, 1996.

Dodson, A.H., P.J. Shardlow, L.C.M. Hubbard, G. Elgered, and P.O.J. Jarlemark, Wet tropospheric effects on precise relative GPS height determination, *J. Geod., 70*, 188–202, 1996.

Dragert, H., and R. D. Hyndman, Continuous GPS monitoring of elastic strain in the northern Cascadia subduction zone, *Geophys. Res. Lett., 22*, 755–758, 1995.

Elgered, G., Tropospheric radio path delay from ground-based microwave radiometry, in *Atmospheric Remote Sensing by Microwave Radiometry*, edited by M. Janssen, pp. 215–258, John Wiley, New York, 1993.

Elgered, G., J.L. Davis, T.A. Herring, and I.I. Shapiro, Geodesy by radio interferometry: Water vapor radiometry for estimation of the wet delay, *J. Geophys. Res., 96*, 6541–6555, 1991.

Emardson, T.R., G. Elgered, and J.M. Johansson, Three months of continuous monitoring of atmospheric water vapor with a network of Global Positioning System receivers, *J. Geophys. Res., 103*, 1807–1820, 1998.

England, M.N., F.J. Schmidlin, and J.M. Johansson, Atmospheric moisture measurements: A microwave radiometer–radiosonde comparison, *IEEE Trans. Geosci. Remote Sens., GE-31*, 389–398, 1993.

Gaffen, D.J., W.P. Elliott, and A. Robock, Relationships between tropospheric water vapor and surface temperature as observed by radiosondes, *Geophys. Res. Lett., 19*, 1839–1842, 1992.

Hogg, D.C., F.O. Guiraud, J.B. Snider, M.T. Decker, and E.R. Westwater, A steerable dual channel microwave radiometer for measurement of water vapor and liquid in the troposphere, *J. Appl. Meteorol., 22*, 789–806, 1983.

Jarlemark, P.O.J., Microwave radiometry for studies of variations in atmospheric water vapor and cloud liquid content, Licentiate thesis, *Tech. Rep. 181L*, School of Electr. and Comput. Eng., Chalmers Univ. of Technol., Göteborg, Sweden, 1994.

Jarlemark, P.O.J., J.M. Johansson, and T.R. Carlsson, Wet delay variability calculated from radiometric measurements and its role in space geodetic parameter estimation, *Radio Sci.*, this issue.

Johansson, J.M., A study of precise position measurements using space geodetic systems, Ph.D. thesis, *Tech. Rep. 229*, School of Electr. and Comput. Eng., Chalmers Univ. of Technol., Göteborg, Sweden, 1992.

Johansson, J.M., G. Elgered, and J.L. Davis, Wet path delay algorithms using microwave radiometer data, in *Contributions of Space Geodesy to Geodynamics: Technology, Geodyn. Ser.*, vol. 25, edited by D.E. Smith and D.L. Turcotte, pp. 81–98, AGU, Washington D. C., 1993.

Liebe, H.J., Atmospheric spectral properties between 10 and 350 GHz: New laboratory measurements and models, in *Proceedings of the Specialist Meeting on Microwave Radiometry and Remote Sensing Applications*, edited by E.R. Westwater, pp. 189–196, Wave Propagation Laboratory, NOAA, Boulder, 1992.

Niell, A.E., Global mapping functions for atmosphere delay at radio wavelengths, *J. Geophys. Res., 101*, 3227–3246, 1991.

Rasool, S.I., and C. De Bergh, The runaway greenhouse and the accumulation of CO_2 in the Venus atmosphere, *Nature, 226*, 1037–1039, 1970.

Raval, A., and V. Ramanathan, Observational determination of the greenhouse effect, *Nature, 342*, 758–761, 1989.

Rind, D., E.-W. Chiou, W. Chu, J. Larsen, S. Oltmans, J. Lerner, M.P. McCormick, and L. McMaster, Positive water vapour feedback in climate models confirmed by satellite data, *Nature, 349*, 500–503, 1991.

Tsuji, H., Y. Hatanaka, T. Sagiya, and M. Hasimoto, Coseismic crustal deformation from the 1994 Hokkaido-Toho-Oki earthquake monitored by a nationwide continuous array in Japan, *Geophys. Res. Lett., 22*, 1669–1672, 1995.

Wade, C.G., An evaluation of problems affecting the measurement of low relative humidity on the United States radiosonde, *J. Atmos. Oceanic Technol., 11*, 687–700, 1994.

Waters, J.W., Absorption and emission by atmospheric gases, in *Methods of Experimental Physics*, vol. 12B, edited by M.L. Meeks, pp. 142–176, Academic, San Diego, Calif., 1976.

G. Elgered, Onsala Space Observatory, Chalmers University of Technology, 439 92 Onsala, Sweden. (e-mail: kge@oso.chalmers.se)

P. O. J. Jarlemark, Harvard-Smithsonian Center for Astrophysics, 60 Garden Street/MS 42, Cambridge, MA 02138. (e-mail: pjarlemark@cfa.harvard.edu)

(Received March 12, 1997; revised February 6, 1998; accepted February 10, 1998.)